

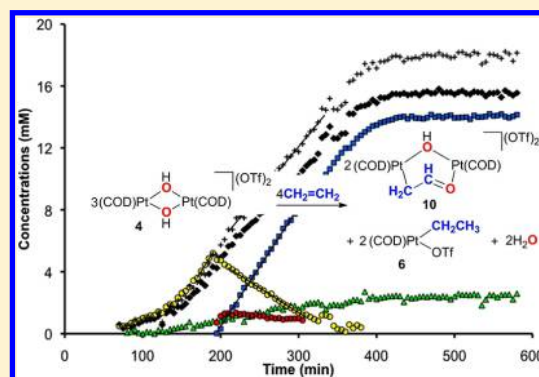
Ethylene Oxidation by a Platinum(II) Hydroxo Complex. Insights into the Wacker Process

Nandita M. Weliange and Paul R. Sharp*

125 Chemistry, University of Missouri—Columbia, Columbia, Missouri 65211, United States

Supporting Information

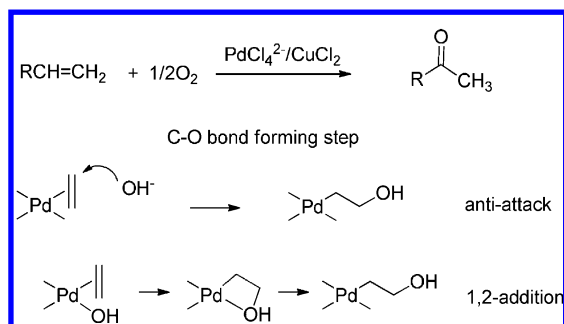
ABSTRACT: The ethylene reaction of hydroxo complex $[\text{Pt}(\text{COD})(\mu\text{-OH})_2(\text{OTf})_2]$ (**4**) yields acetaldehyde and an equilibrium mixture of $\text{Pt}(\text{COD})(\text{C}_2\text{H}_5)(\text{OTf})$ (**6**) and $[\text{Pt}(\text{COD})(\text{C}_2\text{H}_5)(\eta^2\text{-C}_2\text{H}_4)]\text{OTf}$ (**7**). Dinuclear $[\text{Pt}_2(\text{COD})_2(\mu\text{-OH})\{\mu\text{-}\kappa^2\text{C,O-CH}_2\text{C(O)H}\}](\text{OTf})_2$ (**10**) and mononuclear $\text{Pt}(\text{COD})(\text{CH}_2\text{C(O)H})(\text{OTf})$ (**11**) are detected as intermediates during the reaction. The reaction displays three phases: (1) an induction period, (2) an accelerating reaction yielding intermediate **11**, water, and **6** plus **7**, and (3) a linear decrease in the concentration of **11** with simultaneous formation of acetaldehyde and more **6** plus **7**. The reaction is proton catalyzed, and phases 1 and 2 are attributed to autocatalytic behavior resulting from the acidic complex of **6** with water, $[\text{Pt}(\text{COD})(\text{C}_2\text{H}_5)(\text{OH}_2)]\text{OTf}$. Phase 3 is initiated by the complete consumption of basic **4** and the resulting release of protons to catalyze the reaction of **11** with water and ethylene to give acetaldehyde and **6** plus **7**.



INTRODUCTION

Wacker catalytic alkene oxidation has been an important reaction for more than half a century. Originally developed as an aqueous Pd/Cu system with molecular oxygen as the terminal oxidant (Scheme 1),^{1–3} various modified forms of the

Scheme 1



reaction have evolved using different solvents, single metals (Rh, Pt, Pd), and terminal oxidants other than molecular oxygen.^{4–6} An overall mechanism for the classic version has generally been accepted, but uncertainty remains over the C–O bond-forming step (hydroxypalladation)⁷ and subsequent rearrangement processes.^{8,9}

Two commonly considered possibilities for the C–O bond forming step are (Scheme 1) (1) anti attack of an external nucleophilic oxygen species (water or OH^-) on the coordinated alkene (anti addition) and (2) 1,2-addition of the coordinated alkene to the M–O bond of a coordinated OH group (syn addition). In analogy to hydride and alkyl migratory

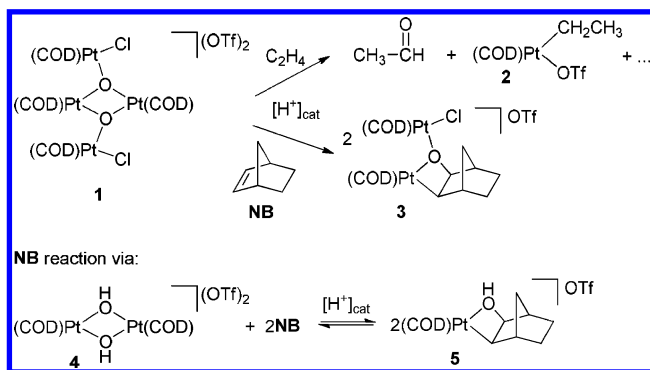
insertion reactions, the product of the addition is often drawn with the OH group dissociated from the palladium center. However, it seems likely that the OH group would remain coordinated to give a protonated metallaioxetane,^{10,11} as shown in Scheme 1. Mechanistic evidence for both possibilities 1 and 2 has been gathered experimentally^{12–23} and computationally,^{7,10,24–31} and it appears that either one may occur depending on reaction conditions and substrate.^{10,21,22}

Various reactions and complexes that may serve as models for the steps and intermediates in the Wacker reaction have appeared in the literature.^{32–57} Some time ago we reported stoichiometric ethylene oxidation to acetaldehyde by Pt(II) oxo complex **1** and formation of platinaoxetane **3** from the reaction of the strained alkene norbornene (NB) with **1** (Scheme 2) and suggested this system as a model for 1,2-addition in Wacker alkene oxidation.^{58,59} Since then we have traced the reactivity of oxo complex **1** to hydroxo complex $[\text{Pt}(\text{COD})(\mu\text{-OH})_2(\text{OTf})_2]$ (**4**)^{60,64} and reported the proton-catalyzed reaction of **4** with NB (Scheme 2).^{60,65} The 1,2-addition of NB to the Pt–OH bond of **4** is rapid and reversible. (For other alkene 1,2-additions to Pt–OH bonds see refs 57 and 66.) Here, we report the reaction of **4** with the simple unstrained alkene ethylene. The reaction displays unusual characteristics, including an induction period and intermediates on the way to the final acetaldehyde product. Modifications to the initial reaction conditions and a study of the intermediates have given insight into the reaction pathway.

Received: July 5, 2012

Published: September 20, 2012

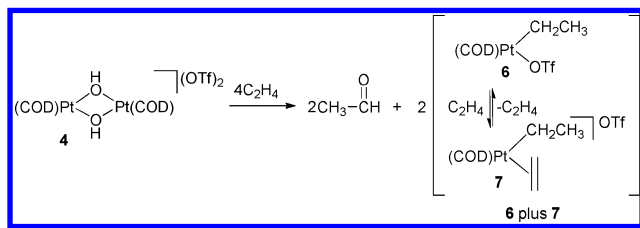
Scheme 2



RESULTS

Reaction Products. Ethylene addition to $[\text{Pt}(\text{COD})-(\text{OH})_2][\text{OTf}]_2$ (**4**) in CD_2Cl_2 causes the colorless solution to become pale yellow after several hours (~ 2 h), ultimately (~ 8 h) yielding acetaldehyde and an equilibrium mixture of $\text{Pt}(\text{COD})(\text{C}_2\text{H}_5)(\text{OTf})$ (**6**) and $[\text{Pt}(\text{COD})(\text{C}_2\text{H}_5)(\eta^2-\text{C}_2\text{H}_4)]\text{OTf}$ (**7**)^{58,67} (Scheme 3). While **6** or **7** could not be

Scheme 3



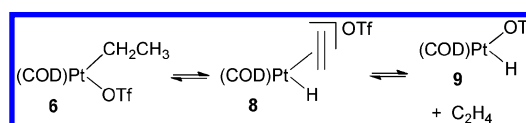
isolated, they were readily identified by their NMR spectra and by independent synthesis. The yield of acetaldehyde (by NMR) varies depending on reaction conditions (see below) but can reach nearly 100%. The yield of **6** plus **7** is essentially quantitative (by NMR), with no other Pt-containing products at the end of the reaction. (Helfer and Atwood have observed similar products in the aqueous phase ethylene reaction of water-soluble *cis*- $\text{PtCl}_2(\text{TPPTS})_2$ (TPPTS = $\text{P}(m\text{-C}_6\text{H}_4\text{SO}_3\text{Na})_3$).⁵⁴)

Acetaldehyde is easily identified by its characteristic quartet (δ 9.75) and doublet (δ 2.15) in the ^1H NMR spectrum of the mixture. Ethyl complex **6** is identified from the close resemblance of its ^1H NMR signals to those of the known chloro analogue, $\text{Pt}(\text{COD})(\text{C}_2\text{H}_5)(\text{Cl})$.⁵⁸ Upfield triplet and quartet patterns with Pt satellites at δ 1.54 and 0.89 indicate the presence of the Pt-bonded ethyl group, while downfield multiplets with differing Pt coupling constants of 23 (trans to Et group) and 97 Hz (trans to OTf) at δ 5.81 and 4.31 account for the olefinic portion of the COD ligand. A ^{195}Pt NMR signal is observed for **6** at δ -3471 . Identical NMR spectra are observed for **6** prepared from $\text{Pt}(\text{COD})(\text{C}_2\text{H}_5)_2$ and HOTf. The known ethyl ethylene complex **7** was also easily identified from its ^1H NMR spectrum.^{58,67} The ethyl group quartet and triplet patterns of **7** appear at unusually high field shifts of δ 0.31 and -0.41 .

Equilibrium between **6** and **7** is evident from the formation of a mixture of **6** and **7** when ethylene is added to a solution of **6** (prepared from $\text{Pt}(\text{COD})(\text{C}_2\text{H}_5)(\text{Cl})$ and AgOTf or from $\text{Pt}(\text{COD})(\text{C}_2\text{H}_5)_2$ and HOTf). Consistent with the ionic formulation of **7**, the equilibrium constant appears sensitive

to the presence of water and other polar species in the mixture, which favor **7**. In fact, in the presence of 1 equiv of HOTf only **7** is observed.⁶⁷ (Water displacement of OTf^- from **6** is also a possible factor in the equilibrium: see below and Scheme 6.) Unlike **6**, which decomposes in hours, the **6**, **7**, and ethylene mixture is stable for days. EXSY spectroscopy (1200 ms mixing time) on the mixture reveals an additional equilibrium. The free ethylene peak at δ 4.85 is correlated with the ethyl CH_3 peak of **6** at δ 0.89, and the CH_2 and the CH_3 peaks of the ethyl group are correlated to each other, although a strong COSY correlation between the CH_2 and the CH_3 peaks make it difficult to be certain of the EXSY correlation. These correlations indicate exchange through reversible β -hydride elimination to ethylene hydride complex **8** and ethylene exchange, possibly through **9** (Scheme 4). Careful examination

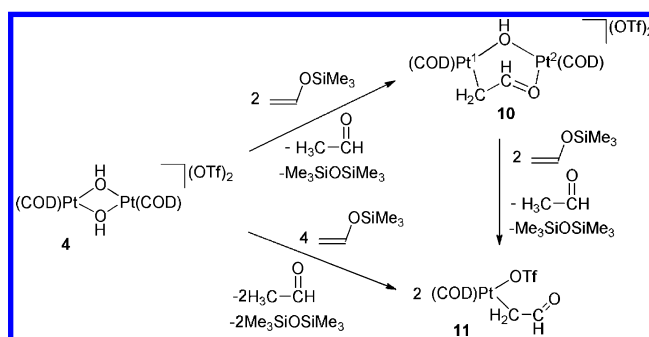
Scheme 4



of the high-field region of the ^1H NMR spectrum of the mixture revealed a small singlet at δ -1.96 with Pt satellites ($J_{\text{Pt-H}} = 775.5$ Hz) that can be assigned to the hydride ligand of **8** or **9**. Similar systems relating metal hydride, alkyl, and olefin complexes have been reported or proposed for Pt,^{68,69} Pd,^{70,71} and Ni^{72,73} complexes involved in olefin oligomerizations.

Intermediates. Monitoring the reaction of **4** and ethylene revealed two intermediates, dinuclear $[\text{Pt}_2(\text{COD})_2(\mu\text{-OH})\{\mu\text{-}\kappa^2\text{C}_2\text{O}-\text{CH}_2\text{C}(\text{O})\text{H}\}](\text{OTf})_2$ (**10**) and mononuclear $\text{Pt}(\text{COD})(\text{CH}_2\text{C}(\text{O})\text{H})(\text{OTf})$ (**11**). These complexes are unstable to isolation but were identified by their NMR spectral signatures and by independent synthesis. Thus, both **10** and **11** are also produced in the reaction of hydroxo complex **4** with (vinylxy)trimethylsilane according to Scheme 5. (Related

Scheme 5



complexes have been similarly prepared.^{32,34,50}) Hydroxo complex **4** is poorly soluble, making it difficult to prevent the first formed and freely soluble **10** from reacting further with (vinylxy)trimethylsilane to give **11**. As a result, we were unable to obtain pure samples of **10**; some **11** is always present. Pure solutions of **11** can be obtained with 6 equiv or more of (vinylxy)trimethylsilane. This is more than the 4 equiv required by the stoichiometry, and the excess is presumably needed because of the reaction of (vinylxy)trimethylsilane with adventitious water in the reaction mixture.

Proton NMR assignments and NOE correlations for **10** are given in Figure 1. A prominent feature in the ^1H NMR

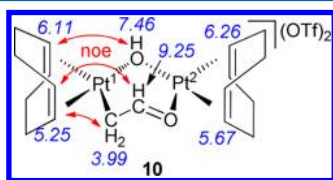


Figure 1. ^1H NMR assignments and noe correlations for **10**.

spectrum of **10** is the aldehydic proton of the bridging formylmethyl ($\mu\text{-}\kappa^2\text{C,O-CH}_2\text{C(O)H}$) ligand, observed in CDCl_3 as a triplet at δ 9.25, in the same range reported for nonbridging formylmethyl complexes.^{32,34,38,45,50,52,74} Samples of **10** display broad and variable ^{195}Pt satellites for the aldehydic peak. This behavior is associated with an equilibrium process involving **11** (see below). The ^{13}C NMR peak for the carbonyl carbon atom (correlated to the aldehydic peak in the $^1\text{H-}^{13}\text{C}$ HMQC spectrum) is found at δ 208.9, downfield from that of acetaldehyde at δ 200 and in the same range as the carbonyl carbon atom of bridging ketonyl ligands^{75–77} and also in the range for nonbridging formylmethyl complexes.^{32,34,38,45,50,52,74} Aldehydic proton coupling to ^{195}Pt is clearly resolved in the $^1\text{H-}^{13}\text{C}$ HMQC spectrum, giving a surprisingly large coupling constant of 286 Hz. The methylene protons of the $\mu\text{-}\kappa^2\text{C,O-CH}_2\text{C(O)H}$ ligand were assigned from a COSY experiment where a doublet at δ 3.99 ($J_{\text{Pt-H}} = 73.0$ Hz) correlates to the aldehydic peak at δ 9.25. Again, this shift is in the region observed for formylmethyl^{32,34,38,45,50,52,74} and related ketonyl ($-\text{CH}_2\text{C(O)R}$) ligands.^{75,76,78–84} $^1\text{H-}^{195}\text{Pt}$ HMQC spectroscopy (Table 1) shows correlation of the methylene protons to a

Table 1. $^1\text{H-}^{195}\text{Pt}$ HMQC Spectroscopy Correlations for **10** and **11**

^{195}Pt NMR signal (ppm)	correlated ^1H NMR signal (ppm)
–3065 (10)	9.25, 6.26, 5.67, ~2.3
–3410 (10)	6.11, 5.25, 3.99, ~2.3
–3342 (11)	4.85, 2.84, ~2.3

Pt signal at δ –3410 (assigned to Pt^1 in Figure 1), while the aldehydic proton is correlated to an equal-intensity Pt signal at δ –3065 (assigned to Pt^2 in Figure 1). Thus, $^1\text{H-}^{195}\text{Pt}$ coupling of the aldehydic proton is through the H-C=O-Pt^2 linkage, establishing the bridging character of the formylmethyl ligand. This appears to be the first example of a bridging formylmethyl ligand. Several dinuclear Pd(II) complexes with bridging ketonyl ligands are known, and three have been structurally characterized.^{75–77,85}

The bridging hydroxo group of **10** appears as a singlet at δ 7.46, near that for the parent μ -hydroxo complex **4**. Its identity as an OH group is supported by the $^1\text{H-}^{13}\text{C}$ HMQC spectrum, in which a correlating ^{13}C signal is absent, and by the signal's disappearance with the addition of 1 drop of D_2O . The four olefinic protons of **10** are found at δ 6.26, 6.11, 5.67, and 5.25 with only the two at δ 6.11 and 5.25 displaying coupling to the ^{195}Pt nucleus of 34.5 and 68.0 Hz, respectively. $^1\text{H-}^{195}\text{Pt}$ HMQC spectroscopy reveals them to belong to the COD ligand of Pt^1 , the Pt center that is bonded to the formylmethyl ligand carbon atom. On the basis of the greater trans influence^{78,86} afforded by alkyl groups, the signal at δ 6.11 ($J_{\text{Pt-H}} = 34.5$ Hz) is assigned to the olefinic group trans to the

carbon atom and the signal at δ 5.25 ($J_{\text{Pt-H}} = 68.0$ Hz) to that trans to the $\mu\text{-OH}$ group.⁸¹ This assignment is confirmed from the NOESY spectrum, which shows NOE correlation of the COD signal at δ 6.11 with that of the $\mu\text{-OH}$ group and correlations of the COD signal at δ 5.25 with those of the formylmethyl ligand protons (Figure 1).

The second set of COD signals at δ 6.26 and 5.67 in **10** appear as broad singlets without visible Pt satellites at 27 °C. These are assigned to the olefinic protons of Pt^2 , the Pt center bonded to the formylmethyl ligand oxygen atom, and this is confirmed by $^1\text{H-}^{195}\text{Pt}$ HMQC spectroscopy. Cooling the ^1H NMR sample and probe to 0 °C caused the Pt^2 COD olefinic signals to sharpen and Pt satellites to appear. The Pt coupling constants of 73.2 Hz (δ 6.26) and 68.3 Hz (δ 5.67) are relatively large, as expected for the weak trans influence of the $\mu\text{-OH}$ group and the carbonyl group. The signal with the larger coupling constant at δ 6.26 ($J_{\text{Pt-H}} = 73.2$ Hz) is tentatively assigned to the olefinic protons trans to the carbonyl group. Warming the sample to 55 °C causes the two Pt^2 COD signals to coalesce, giving a broad singlet. The sample decomposes at higher temperatures, preventing observation of a fast exchange spectrum. Although **10** and **11** are in slow equilibrium (see below), this does not appear to be the process that exchanges the Pt^2 COD signals. If it were, exchange of the Pt^1 COD signals and the formylmethyl ligand signals of **10** with those of **11** would also be observed. An intramolecular process to exchange only the Pt^2 COD protons must be occurring. One possibility is rotation of the $\text{Pt}^2(\text{COD})$ fragment. Such an exchange process has been proposed for an isoelectronic $\text{Rh}(\text{COD})$ fragment bonded to a weakly donating bidentate ligand (sparteine).⁸⁷ Supporting DFT calculations indicate a low-spin, tetrahedral-like transition state.

The structure of **11** is somewhat less certain, and possible structures are given in Figure 2. The ^1H NMR spectrum of **11**

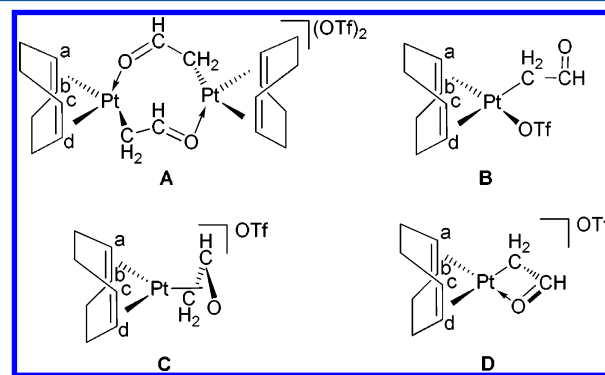


Figure 2. Possible structures for intermediate **11**.

shows an aldehydic proton as a triplet at δ 9.67, near that of dinuclear **10**. However, in contrast to the case for **10**, there is no coupling to Pt in the ^1H NMR spectrum or any correlation with the ^{195}Pt signal in the $^1\text{H-}^{195}\text{Pt}$ HMQC spectrum, which is evidence against dinuclear structure A. COSY spectroscopy shows that the aldehydic triplet is correlated to a doublet with satellites at δ 2.84 ($J_{\text{Pt-H}} = 81.5$ Hz), identifying this as the $\text{CH}_2\text{C(O)H}$ ligand methylene protons. The equivalency of the methylene protons is inconsistent with a static oxoallyl structure (C),^{76,88,89} but a fluxional process involving structure D or B would interchange the protons. The involvement of structure type D has been proposed for fluxional complexes with oxoallyl structures.^{76,89} Unfortunately, at lower temperatures the

methylene signal overlaps with COD peaks and we were unable to determine if its appearance is temperature dependent.

The olefinic signals for **11** appear at δ 5.95 ($J_{\text{Pt-H}} = 30.5$ Hz) and δ 4.85 ($J_{\text{Pt-H}} = 86.5$ Hz) as clear multiplets with Pt satellites. The signal at δ 5.95 is assigned to the olefinic protons trans to the $\text{CH}_2\text{C}(\text{O})\text{H}$ ligand carbon atom, and that at δ 4.85 can be assigned to the olefinic protons trans to the $\text{CH}_2\text{C}(\text{O})\text{H}$ ligand oxygen atom of structure **D** or to the triflate anion of structure **B**. These signals are temperature independent from 25 to 55 °C but at lower temperatures show temperature-dependent shifts, with the δ 5.95 signal shifting upfield to δ 5.86 and the δ 4.85 signal shifting more strongly downfield to δ 5.04 at -50 °C. As the shift is greatest for the olefinic signal (δ 4.85) trans to the weak donor, equilibria between all four structures may be involved and/or coordination of other donor molecules present in the solution (e.g., water and acetaldehyde).

A ^{13}C NMR peak for the carbonyl carbon atom of **11** could not be located, even in mixtures of **10** and **11** where the carbonyl carbon atom of **10** is clearly visible. Presumably, the peak is broadened out from the same equilibria, causing the temperature-dependent olefinic COD ^1H NMR shifts described above. The methylene carbon of the $\text{CH}_2\text{C}(\text{O})\text{H}$ ligand was readily located at δ 37.8. The ^{195}Pt NMR signal (CDCl_3) of **11** is found at δ -3342 and is weaker than would be expected relative to the signals for **10**. The weak signal may again be attributable to the equilibria discussed above. ^1H - ^{195}Pt correlations (Table 1) are observed. The $\text{CH}_2\text{C}(\text{O})\text{H}$ ligand methylene protons at δ 2.84 and the COD olefinic signal at δ 4.85 correlate to the ^{195}Pt NMR signal. A correlation with the COD peak at δ 5.95 (trans to carbon) was not observed, presumably due to the weak coupling to Pt. Also observed in the ^1H - ^{195}Pt HMQC spectrum of both **10** and **11** is a correlation of the Pt signals to a broad COD methylene group signal at $\sim\delta$ 2.3.

Thus, the structure of dinuclear **10** is clearly defined but that of **11** is not and may involve multiple species. However, all are based on the $[\text{Pt}(\text{COD})(\text{CH}_2\text{C}(\text{O})\text{H})]^+$ fragment, which is well represented by structure **B** with its labile coordinated triflate anion, and this structure will be used for all further references to **11**.

Mixtures of **10** and **11** (prepared from **4** and ethylene or from **4** and (vinylxy)trimethylsilane) were studied by EXSY spectroscopy (800 ms mixing time, Table 2). Correlation peaks

Table 2. Exchange in EXSY Spectrum (800 ms Mixing Time) of a CDCl_3 Solution of **10** and **11**

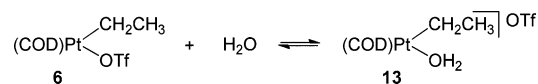
peak for 10	exchange peak ^a
9.25	9.67 (11)
7.46	2.54 (water)
6.26	5.67 (10)
6.11	5.95 (11)
5.25	4.85 (11)
3.99	2.84 (11)

^aPeak assignment given in parentheses.

between the formylmethyl ligand aldehydic and methylene protons and between the COD olefinic protons of **10** and **11** are observed, indicating slow exchange. Of the four olefinic signals for dinuclear **10**, the two olefinic signals for Pt^1 at δ 6.11 and 5.25 exchange with their respective counterparts in mononuclear **11**. The only exchange detected for the two olefinic signals (δ 6.26 and 5.67) for Pt^2 of **10** is with each

other. (This would be expected from the fast fluxional process observed in the VT ^1H MNR spectra of **10** described above.) In addition, the μ -OH group of **10** is in exchange with a very broad (as judged by the correlation peak width) peak at δ 2.5, which is buried under the COD signals. This signal is assigned to water (adventitious or from the formation of **10**), shifted from its usual position of δ 1.56⁹⁰ by coordination to **11** and/or **6** (Scheme 6). D_2O exchange of the OH proton was already noted above.

Scheme 6



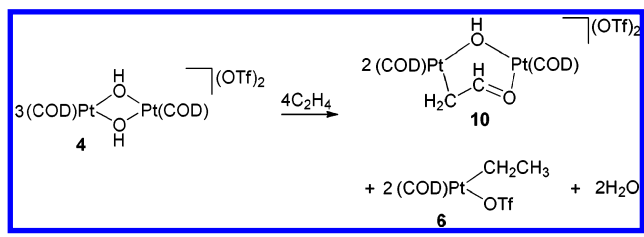
NMR data at various stages of the reaction were also collected at low temperatures (see Table S1 in the Supporting Information). In addition to the ^1H NMR signals for **6**–**11**, two signals were observed at room temperature: a weak unresolved peak at δ 11.4 and a broad moving signal originating at δ 1.52. The signal at δ 11.4 is most intense when **10** is at its highest concentrations (phase 2 to phase 3 transition). The signal is temperature independent and absent at the end of the reaction. The low concentration of the compound and the lack of other visible NMR signals prevented further characterization.

The broad signal at δ 1.52 grows and shifts downfield in the ambient-temperature ^1H NMR spectra during phase 2. Its maximum integrated area occurs at a shift of δ 2.0, coincident in time with the maximum concentration of **10** (phase 2 to phase 3 transition). Subsequently, it is difficult to determine if the area changes, since the signal continues to shift downfield and begins to overlap with the COD methylene signals and eventually entirely overlaps. The signal can be detected up to δ 2.11. Lowering the temperature causes the signal to shift downfield and become visible but also very broad. A CD_3NO_2 reaction displays similar behavior but with the broad signal originating at δ 2.0. Considering the initial chemical shift, the broadness, and the dynamic behavior of this signal, it is assigned to free H_2O (δ 1.52 in CD_2Cl_2)⁹⁰ exchanging with H_2O coordinated to ethyl complex **6** (Scheme 6). Triflate anion displacement by water is a known process,⁹¹ and an equilibrium like that in Scheme 6 has been reported.⁹²

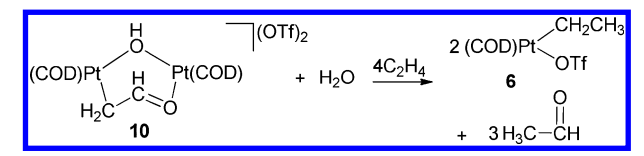
The equilibrium in Scheme 6 also affects the ^{195}Pt NMR spectra. Throughout the reaction, signals for **6** can be seen in the ^1H NMR spectra where coordination of water would have little influence on the COD and ethyl group shifts. However, rapid water coordination and loss should more dramatically affect the ^{195}Pt NMR shifts and room-temperature signals for **6** are absent (exchange broadened) until the reaction is complete and the water peak has disappeared. During the reaction, ^{195}Pt NMR signals observed at δ -3501 and -3539 at -20 and -50 °C are believed to be associated with the aqua ethyl complex **13**. The rise in H_2O concentration along with intermediate **10** and ethyl complex **6** (in equilibrium with **7** and **13**) indicates the stoichiometry of Scheme 7 for phase 2 of the reaction.

Phase 3 of the reaction is marked by the decomposition of intermediate **10**, the formation of acetaldehyde, and the continued production of **6** plus **7**. The ideal stoichiometry for this phase is given in Scheme 8 and requires the consumption of the water produced in phase 2. Phase 3 commences at concentrations of **10** and **6** (plus **7**) that correspond to the complete consumption of hydroxo complex **4** according to

Scheme 7



Scheme 8



Scheme 7 (i.e., at about two-thirds of the starting concentration of 4). Thus, the presence of 4 appears to inhibit the decomposition of 10. This is confirmed by studies of the ethylene reaction of dinuclear intermediate 10 (with some 11) independently prepared from 4 and (vinyloxy)trimethylsilane (see below).

Reaction Variables. To help understand the ethylene reaction of 4, various changes were made to the initial reaction conditions. In the first four experiments (water, HOTf, or Pt(COD)(OTf)_2 addition and reduced ethylene concentration) described below, conditions were held as close as possible to those for the control reaction in Figure 3 (same batch of 4, CH_2Cl_2 solvent, and general procedure).

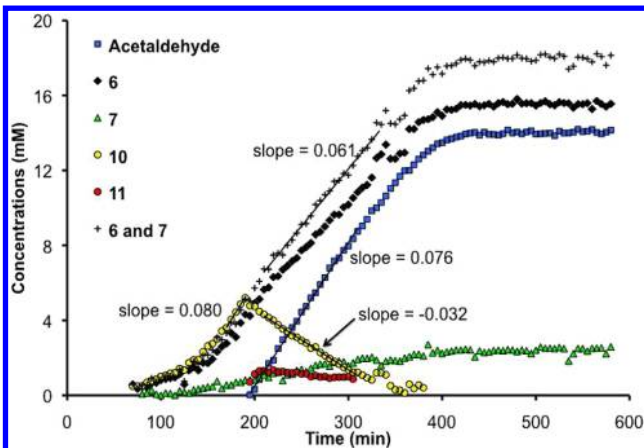


Figure 3. Ethylene reaction profile for $[\text{Pt(COD)(OH)}]_2\text{[OTf]}_2$ (4) in CD_2Cl_2 at 27°C with $[4] = 9 \text{ mM}$ and $[\text{C}_2\text{H}_4] = 200 \text{ mM}$. Slopes are from least-squares fits to linear portions of the plots.

Addition of 10 mol % water (with respect to 4) at the beginning of the reaction has a relatively small effect, causing a slight reduction in the induction period (from ca. 60 to 50 min) and a slight acceleration (10–20%) of the phase 2 and 3 reactions (Figure S1, Supporting Information). In addition, there is a small shift in the equilibrium between ethyl complexes 6 and 7, with ionic 7 being more abundant, probably due to water-induced solvent changes favoring ionic species. A greater concentration of ionic 7 is observed in nitromethane (see below), and only 7 is observed in CD_2Cl_2 in the presence of 1 equiv of HOTf.⁶⁷

In contrast to water, HOTf and Pt(COD)(OTf)_2 additions strongly affect the reaction. Four mole percent HOTf nearly eliminates the induction period, and the phase 2 and 3 reactions are accelerated by a factor of 3–4 (Figure 4).

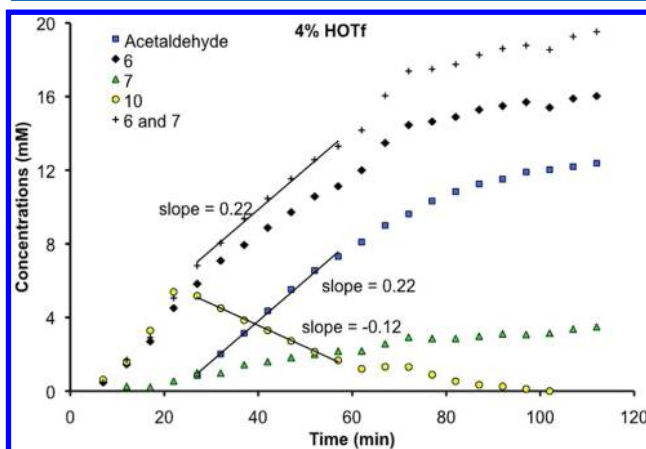


Figure 4. Ethylene reaction profile for $[\text{Pt(COD)(OH)}]_2\text{[OTf]}_2$ (4) in CD_2Cl_2 at 27°C with 4% HOTf, $[4] \approx 9 \text{ mM}$, and $[\text{C}_2\text{H}_4] = 200 \text{ mM}$. Slopes are from least-squares fits to linear portions of the plots.

However, the acetaldehyde yield appears to be reduced from ~80% to ~65%. In a separate set of experiments, ethylene reactions of 4 were run under identical conditions except for added HOTf amounts of 10%, 20%, and 100% (with respect to 4). The respective acetaldehyde yields decreased from 70% to 43% to 17%, respectively. Similar to the case for HOTf, 10 mol % Pt(COD)(OTf)_2 eliminates the induction period (Figure S2, Supporting Information). The phase 2 period is shortened by a factor of 10 from the untreated reaction, and the phase 3 reaction is accelerated by a factor of 4–5. The acetaldehyde yield is reduced to ~70%.

Reducing the ethylene concentration from 200 mM to 56 mM also has a large influence on the reaction (Figure 5). The induction period increases from 50 min to about 200 min, and the phase 2 period extends from a total of 100 min to about 400 min. The phase 3 rate remains similar for the decomposition of 10 and the formation of 6, but the

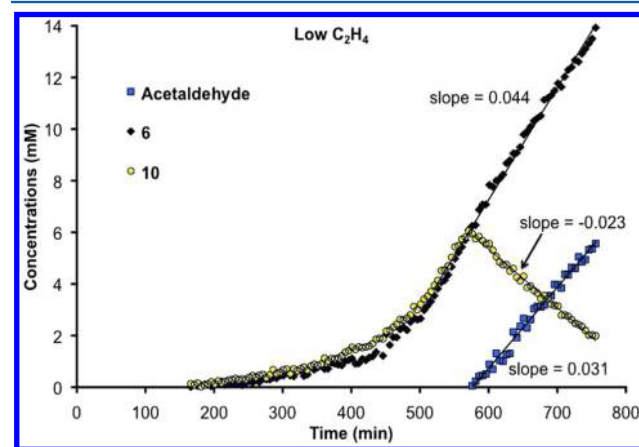


Figure 5. Ethylene reaction profile for $[\text{Pt(COD)(OH)}]_2\text{[OTf]}_2$ (4) in CD_2Cl_2 at 27°C with $[4] = 9 \text{ mM}$ and $[\text{C}_2\text{H}_4] = 56 \text{ mM}$. Slopes are from least-squares fits to linear portions of the plots.

acetaldehyde formation rate is reduced by a factor of about 2, giving a final acetaldehyde yield of only ~50%.

Switching the solvent from CD_2Cl_2 to CD_3NO_2 virtually eliminates the phase 1 induction period and accelerates the phase 2 reaction (Figure S2). The phase 3 decomposition rate of **10** appears similar to that in CD_2Cl_2 , but the acetaldehyde formation rate is reduced, as is the final acetaldehyde yield (~50%). The concentration of **6** could not be monitored during the reaction because the ^1H NMR ethyl peaks of ethyl triflate complex **6** are very broad in CD_3NO_2 and the two olefinic COD peaks of **6**, while sharp, overlap with a COD peak of **10** and the protio residue signal of CD_3NO_2 . Ionic ethyl ethylene complex **7** is observed at somewhat higher concentrations than in CH_2Cl_2 , while the mononuclear intermediate **11** is not seen at all. After 48 h, the known⁹³ allyl complex $[(\text{COD})\text{Pt}(\eta^3\text{-CH}_2\text{CHCHCH}_3)]^+$ is the only Pt-containing product.

Finally, the ability of small amounts of HOTf to nearly eliminate the induction period and speed the reaction suggests proton catalysis. To determine if protons are essential for the reaction, the effect of added polymer-bound diethylamine (~ NET_2) base was tested. Addition of the base at the same time as ethylene to a CD_2Cl_2 solution of **4** causes broadening of the ^1H NMR signals for **4** and a number of new unidentified peaks to appear. Complexes **6**–**11** and acetaldehyde do not form. Base addition in phase 2 of the ethylene reaction of **4** also alters the reaction. When ~ NET_2 is added to a reaction mixture that has progressed to form **6**–**10** and a trace amount of acetaldehyde (beginning of phase 3), then within 30 min ^1H NMR signals of **10** disappear and signals for unknown compound(s) appear. No further acetaldehyde is formed. Also observed is a newly resolved signal at $\delta -1.96$ ($J_{\text{Pt-H}} = 775.5$ Hz), assigned to hydride complex **8** or **9** (Scheme 4). The ^1H NMR spectrum also displays a broad signal at $\delta 1.99$ and a sharp singlet with Pt satellites at $\delta 3.18$ ($J_{\text{Pt-H}} = 56.7$ Hz). ^1H – ^{13}C HMQC reveals the latter to be a Pt-bonded ethylene moiety. The compound to which the ethylene belongs is unknown but may be **8**. After 12 h the signal at $\delta 1.99$ shifts upfield to $\delta 1.87$ and is assigned to the bound water molecule of Pt ethyl aqua complex **13** (see above).

Reaction Chemistry of **10 and **11**.** To gain further insight into phase 3, the reaction chemistry of independently prepared **10** and **11** was investigated. A solution of **10** (with some **11**) was prepared by completely reacting **4** with (vinylxy)-trimethylsilane (Scheme 5). Ethylene addition to this solution resulted in an immediate reaction with formation of acetaldehyde and **6** plus **7**. The reaction profile is given in Figure 6 and resembles that of phase 3 of the ethylene reaction of **4**. However, the amount of acetaldehyde and **6** plus **7** that can form in this reaction is limited by the absence of the water that is generated in phase 2 of the reaction of **4** (see Scheme 7). Only an amount equal to the initial concentration of **10** is observed, suggesting the stoichiometry of Scheme 9 for this reaction. By this stoichiometry, mononuclear intermediate **11** should be a product. While the concentration of **11** does increase at the beginning of the reaction, it does not continue to grow to reach the concentrations of **6** plus **7** and acetaldehyde. No other Pt species is detected, and we are unable to account for the missing Pt-containing product(s).

When the same reaction is run with 10% added HOTf, the final products and amounts are essentially the same as without the added HOTf, but the initial formation rate of acetaldehyde and **6** is about doubled (Figure S4, Supporting Information).

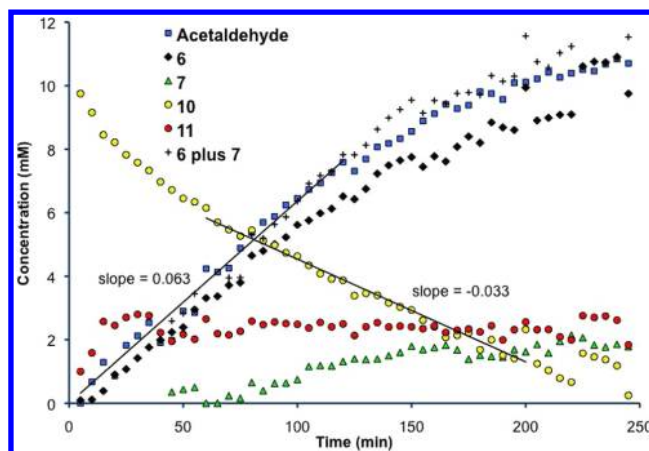
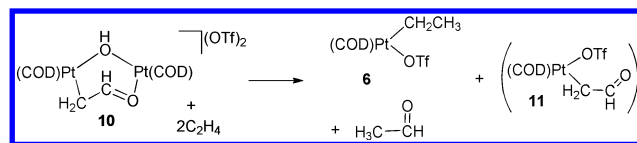


Figure 6. Ethylene reaction profile for a 10:1 mixture of **10** and **11** (prepared in situ from **4** (~9 mM) and (vinylxy)trimethylsilane) in CD_2Cl_2 at 27 °C with $[\text{C}_2\text{H}_4] = 200$ mM. Acetaldehyde from the preparation of **10** has been subtracted. Slopes are from least-squares fits to linear portions of the plots.

Scheme 9



The decay of **10** is also much faster and fits an exponential instead of being approximately linear. This is again consistent with proton catalysis of phase 3.

When **4** is only partially converted to **10** by (vinylxy)-trimethylsilane and the mixture is exposed to ethylene, instead of decreasing, the concentration of **10** increases as remaining **4** is converted to **10** and **6** plus **7** (Figure 7). Only after **4** is completely consumed does **10** begin to decompose, producing acetaldehyde and **6** plus **7** along with small amounts of **11**. In this case, the final yield of **6** plus **7** is quantitative relative to the initial amount of **4** and that of acetaldehyde is 80%.

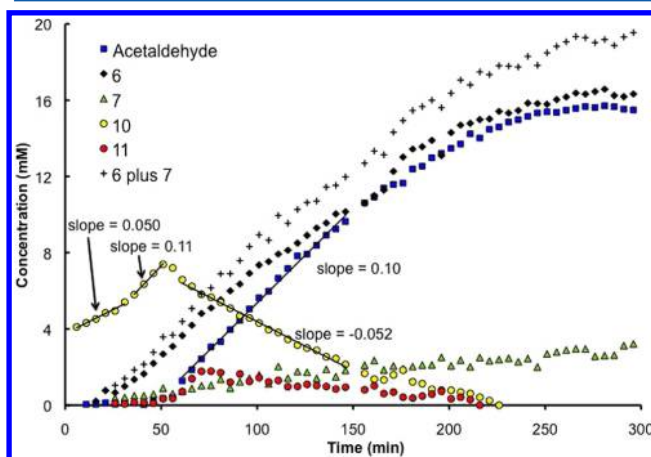
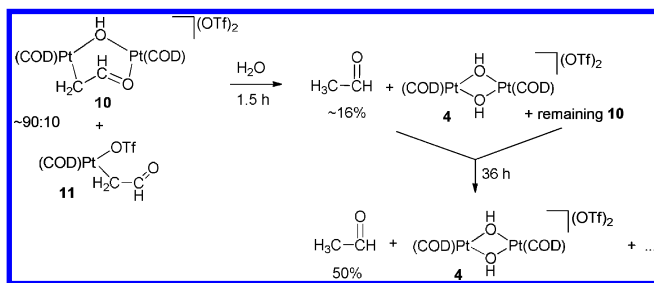


Figure 7. Ethylene reaction profile for a mixture of **4** and **10** (from **4** (~9 mM) and (vinylxy)trimethylsilane) in CD_2Cl_2 at 27 °C with $[\text{C}_2\text{H}_4] = 200$ mM. Acetaldehyde from the preparation of **10** has been subtracted. Slopes are from least-squares fits to linear portions of the plots.

The effect of H₂O on a mixture of **10** and **11**, prepared from (vinylxy)trimethylsilane, was investigated (Scheme 10). To a

Scheme 10

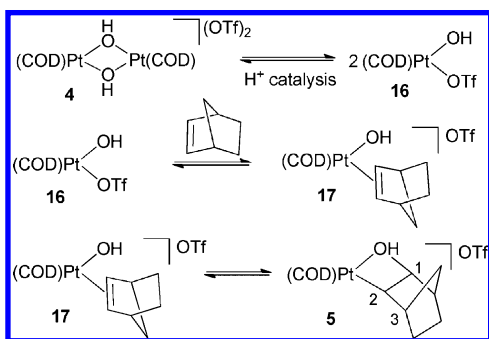


90/10 mixture of **10** and **11** in CD₂Cl₂ was added H₂O (equimolar to the amount of **4** used to prepare the mixture). ¹H NMR spectroscopy indicated acetaldehyde formation (~16% yield based on the sum of **10** and **11**). Signals for mononuclear **11** disappeared, while those for **10** were broadened and slightly decreased. After 1.5 h, ¹H NMR signals for dinuclear **10** further diminished and an olefinic COD signal for hydroxo complex **4** appeared. The ¹⁹⁵Pt NMR spectrum confirmed the presence of **4** and remaining **10**. After 36 h, only signals for acetaldehyde and **4** remained. At this point, the acetaldehyde yield was ~50% (based on the sum of **10** and **11**).

DISCUSSION

The induction period (phase 1) in the ethylene reaction of **4** and the linearity of the reaction profile (zero-order kinetics) over major portions of phases 2 and 3 (Figure 3) suggest reaction catalysis for both the phase 2 and 3 reactions. The dramatic acceleration with catalytic amounts of HOTf (Figure 4) confirms this. Catalysis is also consistent with our previous work on the norbornene (NB) reaction of **4**, which is limited by proton-catalyzed breakup of the hydroxo-bridged structure of **4** and NB trapping of monomer **16** (Scheme 11).⁶⁵

Scheme 11



It would seem reasonable that a similar process would occur for the ethylene reaction and that proton catalysis would also be required. However, ethylene's weaker bonding makes it a much less effective trap for monomer **16** than NB and places greater demands on the catalyst. We believe this is the reason for the induction period in the reaction without added HOTf. Proton impurity levels, while adequate for the NB reaction, are too low to give a significant reaction rate and the induction period involves a buildup of H⁺ concentration. Two scenarios for the induction period in phase 1 and the reaction in phase 2

are considered and can be categorized as autocatalysis and slow catalyst generation.

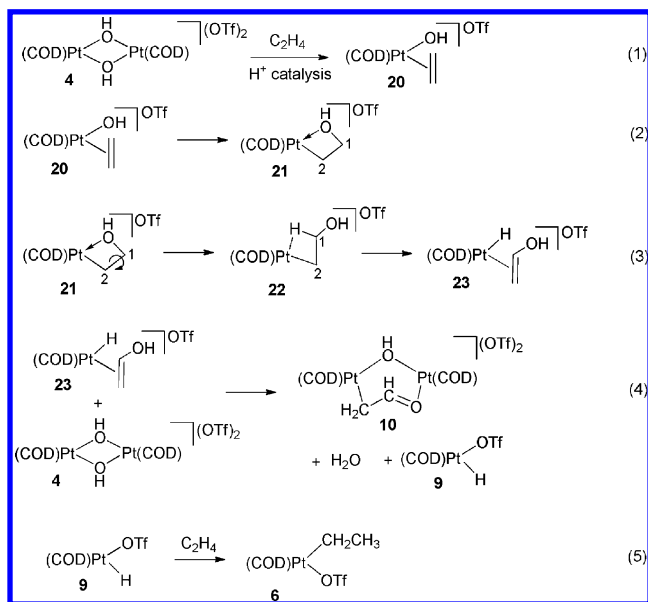
Autocatalysis typically occurs when a product is a catalyst for the reaction or when a product undergoes further reaction to produce a catalyst.^{94–96} Autocatalytic reactions give induction periods and accelerating rates, as observed in phases 1 and 2 (Figure 3). The induction period of an autocatalytic reaction usually involves either a small amount of the catalytic product already present or a slow uncatalyzed reaction which produces a small amount of product to initiate the catalytic reaction.^{97,98} The products over phase 2 of the ethylene reaction of **4** are H₂O, ethyl triflate complex **6**, and dinuclear intermediate **10** (Scheme 7). Water on its own can be eliminated as a catalyst, as it has a relatively small effect on the induction period and the reaction rate when added at the beginning of the reaction (Figure S1). Complex **10** can also be eliminated as a catalyst by the ethylene reaction profile of **4** when **10** is initially present (Figure 7). If **10** were a catalyst, a rapid reaction would be expected instead of the slow initial rate that is observed. We have no data to eliminate ethyl triflate complex **6** as a catalyst, although it is difficult to see how it could be a catalyst on its own. However, **6** is believed to bond water (see above) and the acidic Pt-bonded water molecule would be a proton source. Thus, the combination of **6** and water would be an effective catalyst.

The second possibility we consider is slow proton generation by impurity levels of Pt(COD)(OTf)₂ (**9**). This complex is used to prepare **4** and is known to give HOTf on reaction with ethylene.⁶⁷ Thus, a slow reaction of impurity **9** in the induction period would lead to increasing concentrations of HOTf. The reaction of **9** with ethylene would also explain the lack of an induction period and the acceleration in phase 2 when **9** is added at the beginning of the reaction: higher concentrations of **9** would give faster rates of proton generation. However, **9** also readily adds H₂O, yielding **4** and HOTf (see the Supporting Information). Thus, added **9** and traces of water, as well as water generated in the reaction, would also give H⁺ to catalyze the reaction.

Both of the above scenarios were computer-modeled and fit to the kinetic data of Figure 3 over phases 1 and 2 (see the Supporting Information). Both models give a good fit to the data. However, with reasonable impurity levels of **9** (1–10%) the sensitivity to 4% initial proton concentration of the slow proton generation model is too great and there is no response to initial water. In contrast, the **6** plus water model responds correctly to a 4% initial proton concentration and to a 10% initial water concentration (decreased phase 2 reaction time while leaving the induction period nearly unchanged). Of the two possibilities considered, we therefore favor autocatalysis with H⁺ generated by water coordinated to **6**.

A proposed scheme for the phase 2 reaction pathway is given in Scheme 12. Quite a few steps must occur in this reaction, including the C–O bond forming step, but no intermediates are detected. As with the NB reaction (Scheme 11), a proton-catalyzed breakup of **4** and ethylene coordination yields ethylene hydroxo complex **20** (step 1). The analogous NB hydroxo complex **17** is not observed in the reaction of **4** with NB, but its intermediacy is indicated by the formation of protonated platinaoxetane **5** via syn addition of the coordinated OH group to NB. In analogy, 1,2-addition is proposed in step 2 for the ethylene reaction. However, Vedernikov⁹⁹ reports that Pt(dpms)(OH)(C₂H₄) (dpms = bis(2-pyridyl)-methanesulfonate) in water does not undergo 1,2-addition,

Scheme 12

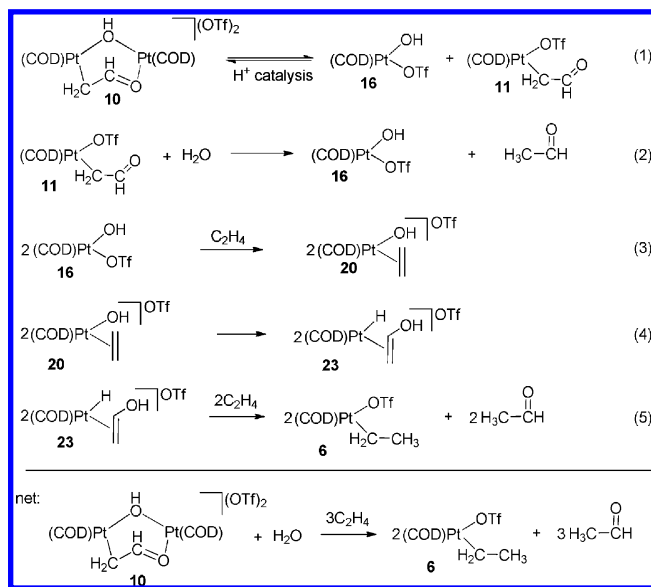


even though the analogous NB and *cis*-cyclooctene complexes do.⁵⁷ $\text{Pt}(\text{dpms})(\text{OH})(\text{C}_2\text{H}_4)$ does undergo reversible anti attack by free OH^- to give the hydroxo hydroxoethyl complex $[\text{Pt}(\text{dpms})(\text{OH})(\text{C}_2\text{H}_4\text{OH})]^-$. Free OH^- attack on the coordinated ethylene of **20** is not reasonable under our reaction conditions, given the nonaqueous solvent and the absence of free OH^- . Water is present and could attack the coordinated ethylene of **20**, but added water has little effect on the phase 2 reaction. Thus, we believe the most reasonable C–O bond forming step is 1,2-addition for ethylene hydroxo complex **20** to give protonated platinaoxtane **21**.

A key difference between the NB reaction and the ethylene reaction is that the NB reaction stops at the formation of protonated platinaoxtane **5**. The ethylene reaction continues on from analogous **21**, ultimately to the oxidized alkene product, acetaldehyde. At least part of the reason for this difference is the rigidity of the NB fragment. After coupling of the alkene and the hydroxo group to form the protonated platinaoxtane, the Pt–OH bond becomes a weak dative bond and dissociation is facile, giving an open coordination site for β -hydride elimination. (β -hydride elimination from a protonated rhodaoxtane has been observed.⁴⁸) In the case of NB platinaoxtane **5**, the rigidity of the ring system prevents rotation about the C1–C2 bond and access of the C1 β -hydrogen atoms to the open coordination site. The C3 β -hydrogen atom does have access but is in a bridgehead position, unfavorable for β -hydride elimination. The more flexible ethylene platinaoxtane **21** can readily rotate about the C1–C2 bond, positioning the C1 β -hydrogen atoms for facile β -hydride elimination in **22** (Scheme 12, step 3). The facile β -hydride elimination, combined with the slower breakup of **4**, results in **21** not being observed. The product of the β -hydride elimination is the vinyl alcohol hydride complex **23**. The vinyl alcohol group of **23** is expected to be acidic,^{32,34} and this complex is also not observed. Instead, it is deprotonated by **4** to form the phase 2 products water, dinuclear intermediate **10**, and ethyl complex **6**, after insertion of ethylene into the Pt–H bond of **9** (Scheme 12, steps 4 and 5).

A proposed pathway for phase 3 of the ethylene reaction, the decomposition of intermediate **10**, is given in Scheme 13. This

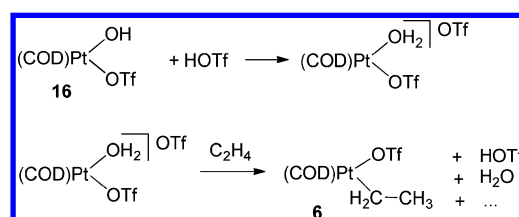
Scheme 13



phase is also proton catalyzed, as evidenced by the linear portions of the reaction profile (Figure 3) and the HOTf acceleration of the decomposition both in the reaction of **4** (Figure 4) and in the decomposition of independently prepared **10** (Figure 6). As such, we believe the stability of **10** in the presence of **4** is due to a preeminent reaction of **4** with H^+ (i.e., **4** is more basic than **10**). Only after the concentration of **4** has been depleted does H^+ become available for catalyzing the breakup of **10** to **11** and hydroxo triflate complex **16** (step 1). Our independent study of solutions of **10** and **11** shows that **11** reacts with water to produce acetaldehyde while **10** is relatively stable to water (step 2). The Pt-containing product from this reaction is expected to be hydroxo triflate complex **16**, which is also produced in the breakup of **10**. Complex **16** reacts with ethylene to give the hydroxoethylene hydride complex **23** (steps 3 and 4). In phase 2 of the reaction, **23** is rapidly trapped by hydroxo dimer **4** to give **10**, but in phase 3 complex **4** has been consumed, allowing an alternative ethylene displacement of the coordinated hydroxoethylene with subsequent rearrangement to acetaldehyde (step 5). Insertion of ethylene into the Pt–H bond then yields **6**.

Finally, the variable yield of acetaldehyde in the ethylene reaction of **4** with always a quantitative yield of **6** plus **7** is explainable. We have previously shown that the ethylene reaction of $\text{Pt}(\text{COD})(\text{OTf})_2$ or $[\text{Pt}(\text{COD})(\text{OTf})(\text{THF})](\text{OTf})$ yields **7** and HOTf.⁶⁷ This suggests the proton-catalyzed reaction shown in Scheme 14, where the aqua complex $[\text{Pt}(\text{COD})(\text{OTf})(\text{H}_2\text{O})](\text{OTf})$ would show reactivity similar to that of the THF complex. Under certain conditions this reaction may operate in parallel with acetaldehyde formation,

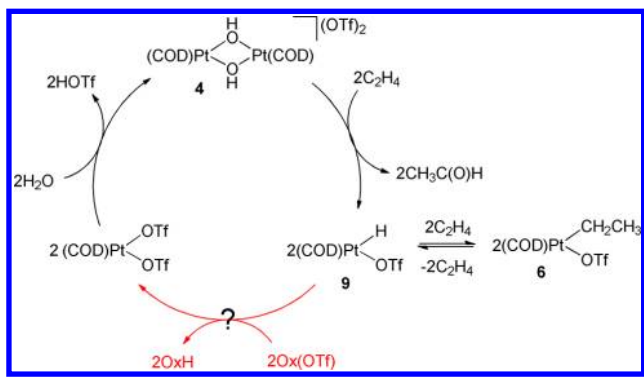
Scheme 14



reducing the acetaldehyde yield without affecting the yield of **6** plus **7**.

Potential Catalytic Cycles. In Pd Wacker and Wacker-like catalytic cycles, product is released through a reductive elimination or a β -hydride elimination, leaving a Pd(0) complex or a Pd(II) hydride complex that must be returned to the electrophilic Pd²⁺ initiator. It is at this step that analogous Pt(II) catalytic cycles often fail.^{54,100} Platinum(II) hydride complexes are more stable and less reactive than the analogous Pd hydride complexes. This limitation has been overcome by using hydride abstractors (e.g., Ph₃C⁺) to regenerate the electrophilic Pt(II) center, and catalytic systems have resulted.^{101–103} Presumably, such an approach would work here to produce a catalytic system (Scheme 15). Pt hydride **9** is

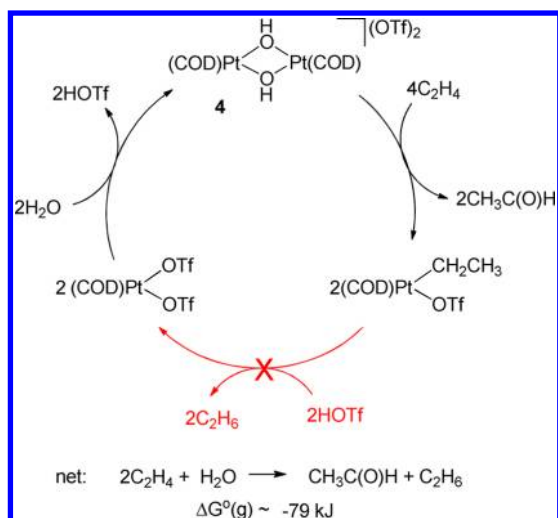
Scheme 15



present in equilibrium with **6** and should be available for hydride abstraction, and we have shown that **4** forms from water and Pt(COD)(OTf)₂ (see the Supporting Information). Unfortunately, this possibility was not recognized until after our work on the alkene reactions of **4** was terminated.

An alternative catalytic cycle that does not involve oxidation of the Pt hydride complex is possible (Scheme 16) if the ethyl group of **6** were more susceptible to protonation.⁶⁷ This reaction is observed for a water-soluble Pt phosphine complex, but the system is slow and is limited to 90 turnovers at 95 °C before catalyst decomposition to Pt black.⁵⁴ Protonation

Scheme 16



resistance of electrophilic Pt alkyl complexes also limits other potential catalytic systems.¹⁰⁰

SUMMARY AND CONCLUSIONS

Complex **4**, under proton catalysis, is remarkably reactive with alkenes. As has been proposed for related systems,¹⁰⁴ protonation most likely disrupts the OH bridge, allowing alkene coordination and activation. The [Pt(COD)(OH)]⁺ fragment is probably particularly effective at alkene activation. An incoming alkene will be trans to a COD π -acceptor olefinic unit, which will minimize back-donation from the Pt center. Although there is no strong evidence for 1,2-addition of the OH group to coordinated ethylene, the analogous norbornene reaction does show 1,2-addition⁶⁰ and most likely it is happening with ethylene as well.

Irrespective of how the C–O bond forms, the subsequent reaction chemistry is fairly complex. As in the Wacker reaction, the hydroxoethyl complex (**21**) undergoes rapid β -hydride elimination. However, rather than rearranging and releasing acetaldehyde, the resulting acidic hydroxoethylene hydride complex **23** is rapidly trapped by basic **4** and more ethylene, allowing the observation of the dinuclear formylmethyl complex intermediate **10**. Only after **4** is consumed does **10** undergo a proton-catalyzed reaction with ethylene and water to release acetaldehyde and form more **6** and **7** and **23**. In the absence of **4**, **23** eliminates acetaldehyde and inserts ethylene to give **6** and **7**. But for one missing step (ethyl group protonation on **6** or hydride oxidation), the reaction would be catalytic.

ASSOCIATED CONTENT

Supporting Information

Text, tables, and figures giving experimental details and NMR data. This material is available free of charge via the Internet at <http://pubs.acs.org>.

AUTHOR INFORMATION

Corresponding Author

*E-mail: sharpp@missouri.edu.

Author Contributions

The manuscript was written through contributions of all authors. All authors have given approval to the final version of the manuscript.

Notes

The authors declare no competing financial interest.

ACKNOWLEDGMENTS

Support from the U.S. Department of Energy, Office of Basic Energy Sciences (DE-FG02-88ER13880) is gratefully acknowledged. We thank Dr. Wei Wycoff for NMR assistance and Dr. Hanbaek Lee for the corannulene sample.

REFERENCES

- (1) Smidt, J.; Hafner, W.; Jira, R.; Sedlmeier, J.; Sieber, R.; Rüttinger, R.; Kojer, H. *Angew. Chem.* **1959**, *71*, 176.
- (2) Tsuji, J. *Palladium reagents and catalysts: New perspectives for the 21st century*, 2nd ed; Wiley: Chichester, U.K., West Sussex, U.K., Hoboken, NJ, 2004.
- (3) Jira, R. *Angew. Chem., Int. Ed.* **2009**, *48*, 9034.
- (4) Takacs, J. M.; Jiang, X.-t. *Curr. Org. Chem.* **2003**, *7*, 369.
- (5) Cornell, C. N.; Sigman, M. S. *Inorg. Chem.* **2007**, *46*, 1903.
- (6) Michel, B. W.; Camelio, A. M.; Cornell, C. N.; Sigman, M. S. *J. Am. Chem. Soc.* **2009**, *131*, 6076.

- (7) Comas-Vives, A.; Stirling, A.; Lledós, A.; Ujaque, G. *Chem. Eur. J.* **2010**, *16*, 8738.
- (8) Beyramabadi, S. A.; Eshtiagh-Hosseini, H.; Housaindokht, M. R.; Morsali, A. *J. Mol. Struct. (THEOCHEM)* **2009**, *903*, 108.
- (9) Keith, J. A.; Oxgaard, J.; Goddard, W. A. *J. Am. Chem. Soc.* **2006**, *128*, 3132.
- (10) Keith, J. A.; Nielsen, R. J.; Oxgaard, J.; Goddard, W. A. *J. Am. Chem. Soc.* **2007**, *129*, 12342.
- (11) Dauth, A.; Love, J. A. *Chem. Rev.* **2011**, *111*, 2010.
- (12) Henry, P. M. *J. Am. Chem. Soc.* **1964**, *86*, 3246.
- (13) Stille, J. K.; James, D. E. *J. Organomet. Chem.* **1976**, *108*, 401.
- (14) Kosaki, M.; Isemura, M.; Kitaura, Y.; Shinoda, S.; Saito, Y. *J. Mol. Catal.* **1977**, *2*, 351.
- (15) Baeckvall, J. E.; Akermark, B.; Ljunggren, S. O. *J. Am. Chem. Soc.* **1979**, *101*, 2411.
- (16) Stille, J. K.; Divakaruni, R. *J. Organomet. Chem.* **1979**, *169*, 239.
- (17) Gregor, N.; Zaw, K.; Henry, P. M. *Organometallics* **1984**, *3*, 1251.
- (18) Zaw, K.; Lautens, M.; Henry, P. M. *Organometallics* **1985**, *4*, 1286.
- (19) Wan, W. K.; Zaw, K.; Henry, P. M. *Organometallics* **1988**, *7*, 1677.
- (20) Hamed, O.; Henry, P. M. *Organometallics* **1997**, *16*, 4903.
- (21) Hamed, O.; Thompson, C.; Henry, P. M. *J. Org. Chem.* **1997**, *62*, 7082.
- (22) Hamed, O.; Henry, P. M.; Thompson, C. *J. Org. Chem.* **1999**, *64*, 7745.
- (23) Nelson, D. J.; Li, R.; Brammer, C. *J. Am. Chem. Soc.* **2001**, *123*, 1564.
- (24) Backvall, J.-E.; Bjorkman, E. E.; Pettersson, L.; Siegbahn, P. *J. Am. Chem. Soc.* **1984**, *106*, 4369.
- (25) Fujimoto, H.; Yamasaki, T. *J. Am. Chem. Soc.* **1986**, *108*, 578.
- (26) Siegbahn, P. E. M. *J. Am. Chem. Soc.* **1995**, *117*, 5409.
- (27) Siegbahn, P. E. M. *J. Phys. Chem.* **1996**, *100*, 14672.
- (28) Kragten, D. D.; van Santen, R. A.; Lerou, J. J. *J. Phys. Chem. A* **1999**, *103*, 80.
- (29) DeKock, R. L.; Hristov, I. H.; Anderson, G. D. W.; Göttker-Schnetmann, I.; Mecking, S.; Ziegler, T. *Organometallics* **2005**, *24*, 2679.
- (30) Beyramabadi, S. A.; Eshtiagh-Hosseini, H.; Housaindokht, M. R.; Morsali, A. *Organometallics* **2008**, *27*, 72.
- (31) Keith, J. A.; Nielsen, R. J.; Oxgaard, J.; Goddard, W. A.; Henry, P. M. *Organometallics* **2009**, *28*, 1618.
- (32) Tsutsui, M.; Ori, M.; Francis, J. *J. Am. Chem. Soc.* **1972**, *94*, 1414.
- (33) Cotton, F. A.; Francis, J. N.; Frenz, B. A.; Tsutsui, M. *J. Am. Chem. Soc.* **1973**, *95*, 2483.
- (34) Hillis, J.; Francis, J.; Ori, M.; Tsutsui, M. *J. Am. Chem. Soc.* **1974**, *96*, 4800.
- (35) Abeysekera, A. M.; Grigg, R.; Trocha-Grimshaw, J.; Viswanatha, V. *J. Chem. Soc., Perkin Trans. 1* **1977**, 1395.
- (36) Day, V. W.; Klemperer, W. G.; Lockledge, S. P.; Main, D. J. *J. Am. Chem. Soc.* **1990**, *112*, 2031.
- (37) Fowler, P.; Read, G.; Shaw, J.; Sik, V. *J. Chem. Soc., Dalton Trans.* **1991**, 1087.
- (38) Woerpel, K. A.; Bergman, R. G. *J. Am. Chem. Soc.* **1993**, *115*, 7888.
- (39) Hutson, A. C.; Lin, M.; Basicckes, N.; Sen, A. *J. Organomet. Chem.* **1995**, *504*, 69.
- (40) Basicckes, N.; Hutson, A. C.; Sen, A.; Yap, G. P. A.; Rheingold, A. L. *Organometallics* **1996**, *15*, 4116.
- (41) Hauger, B. E.; Huffman, J. C.; Caulton, K. G. *Organometallics* **1996**, *15*, 1856.
- (42) Hosokawa, T.; Takano, M.; Murahashi, S. I. *J. Am. Chem. Soc.* **1996**, *118*, 3990.
- (43) Ritter, J. C. M.; Bergman, R. G. *J. Am. Chem. Soc.* **1997**, *119*, 2580.
- (44) de Bruin, B.; Boerakker, M. J.; Donners, J. J. M.; Christiaans, B. E. C.; Schlebos, P. P. J.; De Gelder, R.; Smits, J. M. M.; Spek, A. L.; Gal, A. W. *Angew. Chem., Int. Ed. Engl.* **1997**, *36*, 2064.
- (45) Giordano, F.; Ruffo, F.; Saporito, A.; Panunzi, A. *Inorg. Chim. Acta* **1997**, *264*, 231.
- (46) Hosokawa, T.; Nomura, T.; Murahashi, S.-I. *J. Organomet. Chem.* **1998**, *551*, 387.
- (47) Matsumoto, K.; Nagai, Y.; Matsunami, J.; Mizuno, K.; Abe, T.; Somazawa, R.; Kinoshita, J.; Shimura, H. *J. Am. Chem. Soc.* **1998**, *120*, 2900.
- (48) de Bruin, B.; Boerakker, M. J.; Verhagen, J. A. W.; de Gelder, R.; Smits, J. M. M.; Gal, A. W. *Chem. Eur. J.* **2000**, *6*, 298.
- (49) Lin, Y.-S.; Misawa, H.; Yamada, J.; Matsumoto, K. *J. Am. Chem. Soc.* **2001**, *123*, 569.
- (50) De Felice, V.; Giordano, F.; Orabona, I.; Tesauero, D.; Vitagliano, A. *J. Organomet. Chem.* **2001**, *622*, 242.
- (51) de Bruin, B.; Peters, T. P. J.; Thewissen, S.; Blok, A. N. J.; Wilting, J. B. M.; De Gelder, R.; Smits, J. M. M.; Gal, A. W. *Angew. Chem., Int. Ed.* **2002**, *41*, 2135.
- (52) Krom, M.; Coumans, R. G. E.; Smits, J. M. M.; Gal, A. W. *Angew. Chem., Int. Ed.* **2002**, *41*, 575.
- (53) Budzelaar, P. H. M.; Blok, A. N. J. *Eur. J. Inorg. Chem.* **2004**, *2004*, 2385.
- (54) Helfer, D. S.; Atwood, J. D. *Organometallics* **2004**, *23*, 2412.
- (55) Hettterscheid, D. G. H.; Smits, J. M. M.; de Bruin, B. *Organometallics* **2004**, *23*, 4236.
- (56) Tejel, C.; Ciriano, M. A.; Sola, E.; del Río, M. P.; Ríos-Moreno, G.; Lahoz, F. J.; Oro, L. A. *Angew. Chem., Int. Ed.* **2005**, *44*, 3267.
- (57) Khusnutdinova, J. R.; Newman, L. L.; Zavalij, P. Y.; Lam, Y. F.; Vedernikov, A. N. *J. Am. Chem. Soc.* **2008**, *130*, 2174.
- (58) Szuromi, E.; Shan, H.; Sharp, P. R. *J. Am. Chem. Soc.* **2003**, *124*, 10522.
- (59) NB addition to a Au(III) oxo complex: Cinellu, M. A.; Minghetti, G.; Cocco, F.; Stoccoro, S.; Zucca, A.; Manassero, M. *Angew. Chem., Int. Ed.* **2005**, *44*, 6892.
- (60) Weliange, N. M.; Szuromi, E.; Sharp, P. R. *J. Am. Chem. Soc.* **2009**, *131*, 8736. There is ambiguity in the formulation of **4**. In the solid state, **4** is a tetramer, but kinetic data suggest a dimer in solution. In reality, monomer, dimer, trimer, and tetramer are probably all in equilibrium, as has been observed for other Pt(II) hydroxo complexes of the formula $[L_2Pt(OH)_n]^{n+}$.^{61–63} For convenience, we designate solutions of **4** as the usually more abundant dimer.
- (61) Gill, D. S.; Rosenberg, B. *J. Am. Chem. Soc.* **1982**, *104*, 4598.
- (62) Rochon, F. D.; Morneau, A.; Melanson, R. *Inorg. Chem.* **1988**, *27*, 10.
- (63) Appleton, T. G.; Hall, J. R.; Ralph, S. F.; Thompson, C. S. M. *Inorg. Chem.* **1989**, *28*, 1989.
- (64) An analogous Pd hydroxo dimer has been proposed as the active species in a Pd-catalyzed Wacker-type alkene oxidation: ten Brink, G.-J.; Arends, I. W. C. E.; Papadogianakis, G.; Sheldon, R. A. *Appl. Catal., A* **2000**, *194–195*, 435.
- (65) Weliange, N. M. Ph.D. thesis, University of Missouri, 2011.
- (66) Bennett, M. A.; Jin, H.; Li, S. H.; Rendina, L. M.; Willis, A. C. *J. Am. Chem. Soc.* **1995**, *117*, 8335.
- (67) Szuromi, E.; Sharp, P. R. *Organometallics* **2006**, *25*, 558.
- (68) Tempel, D. J.; Johnson, L. K.; Huff, R. L.; White, P. S.; Brookhart, M. *J. Am. Chem. Soc.* **2000**, *122*, 6686.
- (69) Shiotsuki, M.; White, P. S.; Brookhart, M.; Templeton, J. L. *J. Am. Chem. Soc.* **2007**, *129*, 4058.
- (70) Johnson, L. K.; Killian, C. M.; Brookhart, M. *J. Am. Chem. Soc.* **1995**, *117*, 6414.
- (71) Mecking, S.; Johnson, L. K.; Wang, L.; Brookhart, M. *J. Am. Chem. Soc.* **1998**, *120*, 888.
- (72) Choe, S. B.; Kanai, H.; Klabunde, K. J. *J. Am. Chem. Soc.* **1989**, *111*, 2875.
- (73) Svejda, S. A.; Brookhart, M. *Organometallics* **1999**, *18*, 65.
- (74) Carlisle, S.; Matta, A.; Valles, H.; Bracken, J. B.; Miranda, M.; Yoo, J.; Hahn, C. *Organometallics* **2011**, *30*, 6446.

- (75) Veya, P.; Floriani, C.; Chiesivilla, A.; Rizzoli, C. *Organometallics* **1993**, *12*, 4899.
- (76) Ruiz, J.; Rodriguez, V.; Cutillas, N.; Pardo, M.; Perez, J.; Lopez, G. *Organometallics* **2001**, *20*, 1973.
- (77) Vicente, J.; Arcas, A.; Fernández-Hernández, J. M.; Bautista, D. *Organometallics* **2001**, *20*, 2767.
- (78) Appleton, T. G.; Bennett, M. A. *Inorg. Chem.* **1978**, *17*, 738.
- (79) Vicente, J.; Bermudez, M.-D.; Chicote, M.-T.; Sanchez-Santano, M.-J. *J. Chem. Soc., Chem. Commun.* **1989**, 141.
- (80) Vicente, J.; Abad, J. A.; Chicote, M.-T.; Abrisqueta, M.-D.; Lorca, J.-A.; Ramírez de Arellano, M. C. *Organometallics* **1998**, *17*, 1564.
- (81) Klein, A.; Klinkhammer, K. W.; Scheiring, T. J. *Organomet. Chem.* **1999**, *592*, 128.
- (82) Vicente, J.; Arcas, A.; Fernández-Hernández, J. M.; Bautista, D. *Organometallics* **2006**, *25*, 4404.
- (83) Vicente, J.; Arcas, A.; Fernández-Hernández, J. M.; Bautista, D. *Organometallics* **2008**, *27*, 3978.
- (84) Remy, M. S.; Cundari, T. R.; Sanford, M. S. *Organometallics* **2010**, *29*, 1522.
- (85) Vicente, J.; Arcas, A.; Fernández-Hernández, J. M.; Bautista, D.; Jones, P. G. *Organometallics* **2005**, *24*, 2516.
- (86) Appleton, T. G.; Clark, H. C.; Manzer, L. E. *Coord. Chem. Rev.* **1973**, *10*, 335.
- (87) De Crisci, A. G.; Annibale, V. T.; Hamer, G. K.; Lough, A. J.; Fekl, U. *Dalton Trans.* **2010**, *39*, 2888.
- (88) Zuideveld, M. A.; Kamer, P. C. J.; van Leeuwen, P. W. N. M.; Klusener, P. A. A.; Stil, H. A.; Roobeek, C. F. *J. Am. Chem. Soc.* **1998**, *120*, 7977.
- (89) Slough, G. A.; Hayashi, R.; Ashbaugh, J. R.; Shamblin, S. L.; Aukamp, A. M. *Organometallics* **1994**, *13*, 890.
- (90) Fulmer, G. R.; Miller, A. J. M.; Sherden, N. H.; Gottlieb, H. E.; Nudelman, A.; Stoltz, B. M.; Bercaw, J. E.; Goldberg, K. I. *Organometallics* **2010**, *29*, 2176.
- (91) Lawrance, G. A. *Chem. Rev.* **1986**, *86*, 17.
- (92) Hill, G. S.; Yap, G. P. A.; Puddephatt, R. J. *Organometallics* **1999**, *18*, 1408.
- (93) Boag, N. M.; Green, M.; Spencer, J. L.; Stone, F. G. A. *J. Chem. Soc., Dalton Trans.* **1980**, 1200.
- (94) Andres Ordax, F. J.; Arrizabalaga, A. *An. Quim., A: Quim. Fis. Ing. Quim.* **1985**, *81*, 431.
- (95) Perez-Benito, J. F.; Arias, C.; Brillas, E. *An. Quim.* **1991**, *87*, 849.
- (96) Logan, S. R. *Fundamentals of Chemical Kinetics*; Longman: Harlow, U.K., 1996.
- (97) Begum, R. A.; Chanda, N.; Ramakrishna, T. V. V.; Sharp, P. R. *J. Am. Chem. Soc.* **2005**, *127*, 13494.
- (98) Chanda, N.; Sharp, P. R. *Organometallics* **2007**, *26*, 1635.
- (99) Khusnutdinova, J. R.; Zavalij, P. Y.; Vedernikov, A. N. *Organometallics* **2007**, *26*, 2402.
- (100) Chianese, A. R.; Lee, S. J.; Gagné, M. R. *Angew. Chem., Int. Ed.* **2007**, *46*, 4042.
- (101) Cochrane, N. A.; Brookhart, M. S.; Gagné, M. R. *Organometallics* **2011**, *30*, 2457.
- (102) Mullen, C. A.; Campbell, A. N.; Gagné, M. R. *Angew. Chem., Int. Ed.* **2008**, *47*, 6011.
- (103) Mullen, C. A.; Gagné, M. R. *J. Am. Chem. Soc.* **2007**, *129*, 11880.
- (104) Williams, T. J.; Caffyn, A. J. M.; Hazari, N.; Oblad, P. F.; Labinger, J. A.; Bercaw, J. E. *J. Am. Chem. Soc.* **2008**, *130*, 2418.